ANALYSIS OF RECURRENT ANALOG NEURAL NETWORKS

Zdeněk TOBEŠ, Zbyněk RAIDA
Institute of Radio Electronics
Technical University of Brno
Purkyňova 118, 612 00 BRNO
Czech Republic

Abstract

In this paper, an original rigorous analysis of recurrent analog neural networks, which are built from opamp neurons, is presented. The analysis, which comes from the approximate model of the operational amplifier, reveals causes of possible non-stable states and enables to determine convergence properties of the network. Results of the analysis are discussed in order to enable development of original robust and fast analog networks. In the analysis, the special attention is turned to the examination of the influence of real circuit elements and of the statistical parameters of processed signals to the parameters of the network.

Keywords

analog recurrent neural networks, convergence properties, stability, modelling of operational amplifiers

1. Introduction

Artificial neural networks can be characterised as parallel electronic systems, which exhibit the learning ability. Since classical computers work in the sequential way and parallel multi-processor systems are rather expansive, analog versions of neural networks seem to be rather attractive to be used in some applications.

Dealing with the application of artificial neural networks in radio electronics, many possibilities of their use can be found. The networks can be explored for the control of adaptive antennas, they can be applied to the analog signal processing, to the real-time optimization etc. Thanks to the relatively low price and high operation speed of analog neural networks, they are used in the today's radio-electronic applications more and more frequently.

Recurrent neural networks are characterised by the presence of the feedback loops which lead signals from the outputs of the network back into its inputs. These feedback loops are the basis of the learning ability of this type of networks on one hand but they can produce non-stable states of networks on the other hand.

Because of the presence of many feedback loops in the recurrent neural network and because of the use of many operational amplifiers, real properties of which significantly influence parameters of the network, the rigorous analysis of analog recurrent neural networks is rather complicated, and therefore, it has not appeared in the open literature yet. On the other hand, this analysis is necessary to be performed so as robust and fast neural networks can be designed. Therefore, this work was done.

In the second section of the paper, the analog recurrent neural network with the Least Mean Square (LMS) learning algorithm, which is sometimes called the Wang's one, is reviewed. In the third section, the analysis of the Wang's network is performed. Obtained results are discussed in the section four, and on the basis of this discussion, modified versions of the Wang's network, which exhibit high robustness and high operational speed, are developed.

2. Wang's neural network

The Wang's neural network [1] was designed for the solution of simultaneous set of real linear equations

$$\mathbf{A}.\mathbf{v} = \mathbf{b}, \qquad (1)$$

with the matrix and the column vector of coefficients **A**, **b** respectively, and with the column vector of solutions **v**.

If the size of the matrix equation (1) is of the order N then the Wang's neural network consist of N identical parallely connected blocks - neurons (fig.1).

Operation of this network can be described by the following way. In the first step, a random vector **v'** is put into (1) instead of the searched solution. This substitution produces the column vector of errors

$$\mathbf{e} = \mathbf{b} - \mathbf{A}.\mathbf{v}'. \qquad (2)$$

In the second step, the square of the error vector is minimized by changing **v'** in the contra-direction of the gradient $\mathrm{grad}_{\mathbf{v}'}(\mathbf{e}^2)$

$$d\mathbf{v}'/dt = \eta\mathbf{A}^T[\mathbf{b} - \mathbf{A}\mathbf{v}'(t)] = \theta + \mathbf{W}\mathbf{v}', \qquad (3)$$

where $\theta = \eta\mathbf{A}^T\mathbf{b}$, $\mathbf{W} = -\eta\mathbf{A}^T\mathbf{A}$, $\eta>0$ is the learning constant and ^{T} denotes the transpose.

The elements of the matrix **W** are introduced into the neural network in the form of resistors, which are given by the relation

$$R_{i,j} = R_f / |w_{i,j}| \qquad (4)$$

with the feedback resistor R_f depicted in Fig. 1.

Elements of the column vector θ are introduced into the network by use of voltage sources U_{dc} and resistors R_{dc} (Fig. 1), which are related by the expression

$$R_f U_{dc} / R_{dc} = \theta_i \, . \qquad (5)$$

Then, the neuron consists of the summer computing one row of the right-hand side of (3), of the integrator producing v_i', and of the inverter implementing negative elements of the matrix **W** (minus in **W** is substituted by minus in v_i').

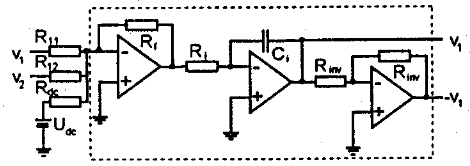

Fig.1 First neuron of the two-dimensional Wang's network

During the transient state, the vector of the initial random solutions **v'** approaches the vector of real solutions of (1) **v**. The time constant of this iteration process can be described by the relation [8]

$$T_i = \frac{\eta}{2 R_i C_i \lambda_i}, \qquad (6)$$

It can be seen that the time constant can be influenced by the learning constant η, which is represented by value of R_f, and by the integration constant $R_i C_i$. Moreover, the settling time depends on eigen-values λ of the matrix **W**.

Trying to obtain as high rate of convergence as possible can yield the instability if real operational amplifiers are used as shown in the next section. Therefore, the stable state with the maximal rate of convergence is useful to be found.

3. Analysis of the Wang's network

The instability of the Wang's network is caused by the high gain of its closed loops as it will be shown later. If the 2-dimensional network is assumed, then three types of closed loops can be found in the system: the first one is inside the model of a real opamp (recursive definition of I_3), the second one is around the opamp using a feedback component (Fig. 1) and the third one is around the neuron. The gain of the last two closed loop is influenced by elements of the matrix **W** (represented by resistors $R_{i,j}$) and by the adaptive parameters of the network (time constants $R_i C_i$ and the learning constant η). Therefore, all these parameters can influence stability of the system. And the question is how they do it.

Answering the question, the ideal opamps in Fig. 1 are replaced by the model of a real opamp [6], which is depicted in Fig. 2.

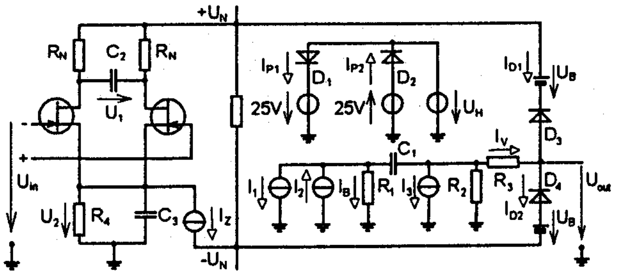

Fig.2 Model of a real operational amplifier

The considered opamp model can be described by the following equations [6]:

$$I_1 = A U_1, \qquad (7)$$

$$I_2 = B U_2, \qquad (8)$$

$$U_H = H I_V, \qquad (9)$$

$$I_3 = C I_B + D I_{P1} - D I_{P2} + E I_{D1} - E I_{D2}, \qquad (10)$$

where A to H are constants and meaning of the rest of symbols can be seen in Fig. 2.

The exact analysis of the two-dimensional Wang's neural network with ideal opamps replaced by their models (Fig. 2) is rather difficult because of the presence of non-linear elements in the circuit (diodes D_1 to D_4).

Dealing with the diodes in the supplying sub-circuit (D_3 and D_4), they does not influence both the stability and the convergence properties of the circuit. This is given by the fact that the current source I_2 and the whole supplying part of the circuit can be neglected because they serve for the non-linear limitation of the output voltage if it approaches the supply voltage. Consequently, if small output voltage is assumed then currents I_{D1} and I_{D2} need not to be considered in (10).

Unfortunately, diodes D_1 and D_2 cannot be neglected even in the closed state which is caused by the role of currents I_{P1} and I_{P2} in the circuit (currents I_{P1} and I_{P2} significantly influences the current I_3 which plays the cardinal role in the stability of the opamp). Therefore, to enable the convergence analysis of the circuit, the diodes D_1 and D_2 are approximated by the linear characteristic in the open state and by an infinite resistance in the closed one.

The possible instability of the circuit is modelled by the current source I_3, which is recursively defined: a part of I_3 consists of the current I_B (10) flowing through the resistor R_1, and regressively, I_B is dependent on the current source I_3 (see Fig. 2). Moreover, there is another recursion in the circuit: a part of the current I_V consists of the current I_3 (see Fig. 2), and regressively, I_V influences the voltage U_H (9). If one of the diodes D_1 or D_2 in Fig. 2 becomes opened then the positive feedback appears in the circuit which can be described by the relation

$$I_3(p) = \frac{I_{31}(p) + \left[I_{32}(p)H - 25D/p\right]\left[1/R_{di1} - 1/R_{di2}\right]}{1 + X(p) + Y(p)\left[1/R_{di1} - 1/R_{di2}\right]}, \quad (11)$$

where

$$I_{31}(p) = -CI_1 \frac{R_1(1 + pC_1R_{ax})}{pC_1(R_1 + R_{ax}) + 1}\frac{1}{R_1} = -I_1 M(p), \quad (12)$$

$$I_{32}(p) = -\frac{pI_1R_1R_{ax}DC_1}{R_{dx}\left[pC_1(R_1 + R_{ax}) + 1\right]} = -I_1 N(p), \quad (13)$$

$$X(p) = C\frac{pR_1R_{ax}C_1}{R_1\left[pC_1(R_1 + R_{ax}) + 1\right]}, \quad (14)$$

$$Y(p) = \frac{(1 + pR_1C_1)R_{ax}HD}{R_{dx}\left[pC_1(R_1 + R_{ax}) + 1\right]}. \quad (15)$$

Further, R_{di1} and R_{di2} denote the resistance of diodes D_1 and D_2, respectively, R_{ax} and R_{dx} are given by the equations (19) and (20), respectively, C and D are constants acting in the equations (7) to (10), H denotes the constant from (9), $p = j\,2\pi f$, and the rest of symbols is explained in Fig. 2.

For simplicity, equation (11) is rewritten to the form

$$I_3(p) = -I_1 K(p) - I_d(p), \quad (16)$$

with

$$I_d(p) = \frac{(25D/p)\left[1/R_{di1} - 1/R_{di2}\right]}{1 + X(p) + Y(p)\left[1/R_{di1} - 1/R_{di2}\right]}, \quad (17)$$

$$K(p) = \frac{M(p) + N(p)H\left[1/R_{di1} - 1/R_{di2}\right]}{1 + X(p) + Y(p)\left[1/R_{di1} - 1/R_{di2}\right]}. \quad (18)$$

Relation (11) expresses description of the current I_3 in the Laplace domain in the situation, when one of diodes D_1 or D_2 is opened (one of resistances R_{di1} or R_{di2} is small), and the output voltage U_{out} diverges.

Further, resistors R_{ax} and R_{dx} playing role in (14) can be expressed as

$$R_{ax} = \frac{R_iR_2(R_f + R_{11}) + R_3R_2(R_f + R_{11} + R_i)}{R_i(R_f + R_{11}) + (R_3 + R_2)(R_f + R_{11} + R_i)}, \quad (19)$$

$$R_{dx} = R_3 + \frac{(R_f + R_{11})R_i}{R_f + R_{11} + R_i}. \quad (20)$$

In the above equations, the resistors R_{11}, R_i and R_f are depicted in Fig.1 and the resistors R_2 and R_3 are depicted in Fig. 2.

In the following step, the above described model of the operational amplifier is substituted into the Wang's neural network. To simplify this task as much as possible, only one neuron with the feedback from its output to the input resistor R_{11} is assumed.

Moreover, in this stage of the analysis, a model of the real operational amplifier is considered being in the summing amplifier only. Dealing with the integrating amplifier and the inverting one, the ideal opamps are considered there. Later, a way of extension of the presented analysis to the case when all the three opamps in the neuron are considered to be real, will be shown in this paper.

All the above described simplifications are necessary to be done because the analysis of the non-simplified circuit leads to high order equations in Laplace domain, solution of which is very difficult.

In the above described circuit, there are two feedbacks from the point of view of voltages on the input of the opamp U_{in} and on its output U_{out}. The first feedback is represented by the feedback resistor R_f in the summing amplifier, and the second one, by the connection between the output of the neuron and the input resistor R_{11} (see Fig.1).

In the first step, the first type of the feedback is handled. For this purpose, the input part of the circuit (the differential amplifier in the opamp) can be described in a rather simple way because both the capacitor C_3 and the current source I_Z can be neglected (I_Z is the constant current which does not influence dynamics of the network, and therefore, is does not influence the stability of the system) and the JFETs can be assumed to work in the linear regime (small signals are assumed to be handled). Then, the transfer function of the input part (relation between the input voltage and the current source I_1) can be expressed as

$$I_1 = \frac{AR_NSU_{in}}{2SR_Np + 1}, \quad (21)$$

where A is the parameter acting in (7), S is the gain of the JFET's transfer characteristics and R_N is depicted in Fig.2.

The output voltage U_{out} representing the error signal in the neuron consists of components U_{out1} and U_{out2} which can be expressed as

$$U_{out1} = -\frac{pR_1C_1R_B}{pR_1C_1 + 1}\frac{R_f + R_a}{R_a}\frac{AR_NSU_{in}}{p2R_nC_2 + 1}, \quad (22)$$

with (23)

$$R_B = \frac{R_2(R_f + R_a + R_i)}{(R_3 + R_2)(R_f + R_a + R_i) + R_i(R_f + R_a)}\frac{R_iR_a}{R_f + R_a + R_i},$$

$$R_a = \frac{R_{11}R_{dc}}{R_{11} + R_{dc}}, \quad (24)$$

and

$$U_{out2} = -R_k \frac{R_f + R_a}{R_a}\left[\frac{AR_N SU_{in}}{p2R_N C_2 + 1}K(p) + I_d(p)\right], \qquad (25)$$

with

$$R_k = \frac{R_2 R_i R_a}{R_3(R_i + R_f + R_a) + R_i(R_f + R_a)}. \qquad (26)$$

Here, I_d is given by (17), K is given by (18), R_i, R_f and R_{11} are depicted in Fig. 1, R_1, R_2, R_3, C_1, C_2 and R_N are depicted in Fig. 2, A is constant acting in (7) and S is the gain of the JFET's transfer characteristics.

Then, the relation between the input voltage of the operational amplifier U_{in} and the output one U_{out} can be expressed as

$$U_{in} = \frac{U_{out}R_a + U_a R_f}{R_a + R_f}. \qquad (27)$$

Substituting (27) into (22) and (25) yields

$$U_{out} = -\frac{U_a Z(p) AR_N SR_f}{(2pR_N C_2+1)R_a + Z(p)AR_N SR_a} - \frac{I_d(p)R_k R_a\left[(R_f+R_a)/R_a\right]\left[2pR_N C_2+1\right]}{(2pR_N C_2+1)R_a + Z(p)AR_N SR_a} \qquad (28)$$

where

$$Z(p) = R_k K(p) + \frac{pR_1 C_1 R_B}{pR_1 C_1 + 1}. \qquad (29)$$

In order to include the second type of the feedback into the analysis, the voltage U_a can be described by the relation

$$U_a = \left(\frac{U_{dc}}{pR_{dc}} + \frac{U_{out}}{pR_{11}R_i C_i}\right)R_a \qquad (30)$$

with U_{dc}, R_{dc}, R_i and C_i being depicted in Fig. 1.

Then, the voltage at the output of the summing opamp U_{out} can be expressed as

$$U_{out} = -\frac{R_{11}R_i C_i}{R_a R_{dc}} \cdot \frac{\left[U_{dc}R_{dc}Z(p)AR_N SR_f + pU_d(p)R_k R_a\right]}{\left[p(2pR_N C_2+1)R_{11}R_i C_i + Z(p)AR_N S(pR_{11}R_i C_i + R_f)\right]} \qquad (31)$$

where

$$U_d = I_d(p)R_{dc}\left[(R_f+R_a)/R_a\right](2pR_N C_2+1). \qquad (32)$$

Finally, eqn. (31) can be rewritten into the form

$$U_{out} = \frac{-R_i C_i(\alpha p^2 + \beta p + \gamma)}{R_i C_i(p^4 + \delta p^3) + (R_i C_i \varepsilon + \varphi)p^2 + (R_i C_i \sigma + \phi)p + \chi} \qquad (33)$$

with α, β, γ denoting coefficients, which can be evaluated according to [10] and which are not important from the point of view of the stability of the system, and with δ, ε, φ, σ, ϕ, χ given by the relations (36) to (40).

Examining the relation (33), several possible forms of the time course of the error signal U_{out} can be found.

The first type of the time course of the error signal exhibits slow convergence without depressed oscillations which is caused by real poles in the denominator of (33).

The second type of the time course of the error signal is convergent with depressed oscillations which is caused by two complex conjugated poles or two pairs of complex conjugated poles in the denominator of (33).

The worst type of the time course of the error signal occurs when diodes become opened and the output voltage of the opamp diverges. In the Laplace domain, one negative pole is obtained in the denominator of (33).

The fourth type of the time course of the error signal corresponds with another undesired state of the circuit: the output signal has the form of sinusoidal divergent signal described by the relation

$$U_{out} = \frac{A}{p^2 + \varpi^2} - \frac{B}{(p+a)^2 + \varpi_1^2}. \qquad (34)$$

with constants A and B being coefficients, which can be evaluated according to [10] and which are not important from the point of view of the stability of the system, with a describing decrease of oscillations, and with ϖ and ϖ_1 being frequencies of oscillations.

Comparing relations (33) and (34) for $\varpi_1 = 0$, a condition for constant oscillations can be found:

$$R_i C_i = \frac{\varphi - \phi/\delta}{(\delta^2/4) + (\sigma/\delta) - \varepsilon} \qquad (35)$$

If the relation (34) is transformed into the time domain then the obtained expression represents the difference between fixed oscillations and depressed ones which corresponds with rising oscillations as the result. These rising oscillations become fixed after certain time, which is given by a parameter a in the relation (34).

Dealing with the relation (35), it shows that the above described states occur in dependence on a gain of the closed loop, i.e. in dependence on C_i, R_i and R_{11} (see relations (36) to (42)). The exact analysis of this dependence is rather difficult because it produces high-order equations. That is why the non-linear sub-circuit containing diodes D_1 and D_2 (see Fig.2) was neglected in the step from (34) to (35) in order to simplify the analysis (currents I_{P1} and I_{P2} in (10) were neglected). In such a case, the divergence of U_{out} can not occur on one hand, but the state described by eqn. (34) (rising oscillations) may arise on the other hand. Then, the symbols in (33) are of the form

$$\chi = \frac{R_{ZV}R_1 AR_N SR_a R_k C}{T(p)}, \qquad (36)$$

$$\phi = \frac{R_1 A R_N S R_a C_1 R_Z \left[R_1 R_B + R_k C(R_1 + R_a + R_{ax})\right]}{T(p)}, \quad (37)$$

$$\varphi = \frac{R_1 A R_N S R_a C_1 \left\{C_1 R_{ZV} \left\{R_k C R_{ax} R_1 + R_B R_1 \left[R_{ax}(1+C) + R_1\right]\right\}\right\}}{T(p)},$$

$$\delta = \frac{\left[R_{ZV} + R_a\right] R_1 R_{11} C_1}{T(p)} \cdot \left\{R_1 2 C_2 R_N + \left[2 C_2 R_N + R_1 C_1\right]\left[R_{ax}(1+C) + R_1\right]\right\} + \frac{R_1 R_{11} R_1 A R_N S R_a}{T(p)} \cdot \left\{2 C_2 R_N + R_1 C_1 + C_1\left[R_{ax}(1+C) + R_1\right]\right\} \quad (39)$$

$$\varepsilon = \frac{R_1 A R_N S R_a R_{11} C_1 \left[R_1 R_B + R_k C(R_1 + R_{ax})\right]}{T(p)} + \frac{(R_{ZV} + R_a) R_1 R_{11} \left\{2 C_2 R_N + R_1 C_1 + C_1\left[R_{ax}(1+C) + R_1\right]\right\}}{T(p)} \quad (40)$$

$$\sigma = \frac{R_1 A R_N S R_a R_{11} R_k C + R_1 R_{11}(R_{ZV} + R_a)}{T(p)} \quad (41)$$

$$T(p) = (R_{ZV} + R_a) R_1 R_{11} C_1^2 R_1 2 C_2 R_N (R_{ax}(1+C) + R_1). \quad (42)$$

Validity of results of the above described analysis of one neuron can be generalised for a neural network consisting of an arbitrary number of neurons [10]: both the error signal U_{out} and all the other variables acting in final expressions have to be considered as vector and matrix variables. Then, the relation (30) is of the form

$$\mathbf{U}_a = \left(\frac{\mathbf{A}^T \mathbf{b}}{p} + \frac{\mathbf{U}_{out} \mathbf{W}}{p R_i C_i}\right), \quad (43)$$

where **A** and **b** are matrix and vector of input signals from (1) and $\mathbf{W} = \eta \mathbf{A}^T \mathbf{A}$.

Substituting (43) into (27) yields the relation for the vector of error signals $\mathbf{U}_{out}$ and new form of the relation (33) is obtained, which depends now on eigenvalues of the matrix of input signals **W**. The matrix of eigenvalues of **W** can be obtained by application of a matrix transformation described in [8].

In the following section, possible electronic implementations of the results of the above described analysis are discussed in order to obtain as robust and as fast as possible modified versions of the classical Wang's neural network.

4. Electronic realisation of results of the analysis

As the most important result of described analysis, mathematical relations for the dependence of the stability and for the convergence rate of the network on the ratio of eigenvalues of matrix **W** (which is represented by resistors R_{ij}) can be considered. Of course, the discussion requires taking the two-dimensional Wang's network in mind at least, which is described by the fifth-order polynomial in the denominator of (33). Then, the following conclusion can be done: If the eigenvalue ratio of **W** equals one then gains of closed loops of each neuron are approximately the same. On the other hand, if the eigenvalue ratio of **W** significantly differs from one, and at the same time, circuit parameters influencing closed loops gains are the same in all neurons case then there is one neuron with small gain (corresponding with the small eigenvalue) on the other one with high gain (corresponding with high eigenvalue). Then, the maximal gain, which can be set in order to keep the stability of the whole network, has to correspond with a maximal possible gain of the high-gain neuron. I.e. parameters influencing closed loops gains must be set proportionally to this maximal gain, and the ratios of both gains is kept. Unfortunately, the neuron with small gain increases the convergence time. The described property is undesired in applications, where the high convergence rate is required.

To overcome the described difficulty, several solutions have been so far proposed.

In [6], an approach of removing the dependence of the system on eigenvalues of W was published. But it came from the mathematical description based on ideal circuit components. This approach exhibited the independence of the convergence rate with respect to the ratio of eigenvalues of **W**. Unfortunately, computer simulations with real opamps showed that this approach fails for the eigenvalue ratios significantly differing from one. Increasing the eigenvalue ratio, closed-loop gain were necessary to be increased also (towards the very large values). In the opposite case, the network produced a big misadjustment due to the inaccurate computation of weights and convergence time is long.

Another approach for obtaining the convergence time independent on the eigenvalue ratio was obtained by the use of the Kalman filter which is independent on the eigenvalue ratio by its nature (of course, ideal opamps must be considered). Unfortunately, the obtained network is rather complicated. Of course, there are some possibilities of simplifying the structure [2], but the price, which must be paid for this, is given by higher dependence of the convergence rate on the eigenvalue ratio. In real conditions, problems of the both pure and simplified Kalman's network are similar to those of Wang's one, but reached convergence rate is much higher.

Another possible approach consists in setting time constants, or other parameters representing the closed-loop gain, separately for each neuron. The time constants are set on the basis of the statistical parameters of input signals so that the neuron with the highest corresponding eigenvalue can be in a stable state and the neuron with the smallest corresponding eigenvalue cannot cause the long convergence time. By this way, the dependence of the circuit on the eigenvalue ratio can be decreased. However, the setting of time constants cannot represent a linear dependence on eigenvalues in real conditions [9] because of possible appearance of an unstable state. Further, it is technically impossible to compute eigenvalues of the correlation matrix in order to set parameters of the circuit in real time. Therefore, an approximate solution of the problem consisting in substituting eigenvalues by numbers in the diagonal of **W** was developed [9], but unfortunately, the high convergence rate was accompanied by possible unstable states. Therefore, an additional circuit [4], which was based on the circuit, which does not fulfil the condition (34) and which consequently eliminated unstable states, had to be added to the system.

Dealing with the verification of all the circuits, described in this section, they were simulated in PSPICE 5.1 with good results.

5. Conclusion

The paper presents an original analysis of the Wang's network with neurons consisting of models of real operational amplifiers. Moreover, the paper shows both the theoretical basis and the implementation possibilities for the development of improvement versions of the network, which excel in the high convergence rate and in good stability.

Because of the enormous complexity of the analysis, the analysed circuit was originally simplified to obtain understandable results on one hand and to preserve convergence properties of the network in the mathematical description on the other hand.

In the first part, the dependence of the stability and of the convergence time of the network on the parameters was proven. Further, previously published improvements were reviewed (Kalman's network, networks of Klemes and Compton), their agreement with the presented theory was discussed and the possible way of the design of robust and fast networks was proposed. The proposed design procedure is based on the control of a separate setting of closed-loop gains of single neurons. The proposed design procedure is similar to the control of the adaptation step in the digital Variable Step-Size LMS algorithm.

References

[1] WANG, J.: "Electronic Realisation of Recurrent Neural Network for Solving Simultaneous Linear Equations", *Electronics Letters*, vol. 28, no. 5, 1992, pp. 493 - 495.

[2] RAIDA, Z : "Improvement of Convergence Properties of Wang's Neural Network", *Electronics Letters*, vol. 30, no. 22, 1994, pp. 1864 - 1866.

[3] TOBEŠ, Z.- RAIDA, Z.: "Stability Problems of Wang's Neural Networks", In: *Proceedings of the National Conference Radioelektronika '96*, TU Brno, Czech Republic, 23. - 24. 4. 1996, pp. 366 - 369.

[4] TOBEŠ, Z.: "Application of Neural Networks in Adaptive Antenna Systems", In: *Proceedings of the International Conference Neural Networks and Their Application Possibilities*, TU Košice, Slovakia, 1996, pp. 107 - 112.

[5] BOYLE, G.- COHN, B.- PEDERSON, D.: "Macro-modelling of Integrated Circuit Operational Amplifiers", *IEEE Journal of Solid - State Circuits*, vol. 9, no. 6, December 1974, pp. 353 - 364.

[6] KLEMES, M.: "A Practical Method of Obtaining Constant Convergence Rates in LMS Adaptive Arrays", *IEEE Transactions on Antennas and Propagation*, vol. 34, no. 3, March 1986, pp. 440 - 446.

[7] WIDROW, B.- MANTEY, P. E.- GRIFFITHS, L. J.- GOODE, B. B.: "Adaptive Antenna Systems", *Proceedings of IEEE*, vol. 55, no. 12, December 1967, pp. 2143 - 2159.

[8] WIDROW, B.- MCCOOL, J. M.: "A comparison of Adaptive Algorithms Based on the Methods of Steepest Descent and Random Search", *IEEE Transactions on Antennas and Propagation*, vol. 24, no. 5, September 1976, pp. 645 - 637.

[9] TOBEŠ, Z.: "Ensuring of Equal Convergence Rates of Analog Neural Networks", In: *Proceedings of the National Conference Radioelektronika '98*, TU Brno, Czech Republic, 28. - 29. 4. '98, accepted for publication.

[10] TOBEŠ, Z.: "*Adaptive Antennas and Their Control by Analog Neural Networks*", Dissertation Thesis, TU Brno, 1998.

About authors...

Zdeněk TOBEŠ was born in Hranice na Moravì (Czech Republic) in 1971. He received the MSc. degree in electrical engineering from VUT Brno, in 1995. At the present time, he is working towards PhD degree at VUT Brno, Institute of Radio Electronics. He is interested in analog neural networks and adaptive antennas.

Zbyněk RAIDA was born in 1967 in Opava. He received Ing. (M.S.) degree in Radio Electronics in 1991 and Dr. (PhD.) degree in Electronics in 1994, both at the Technical University of Brno. Since 1993, he is with the Institute of Radio Electronics VUT Brno where he works as an assistant professor. His research interests include artificial intelligence, numerical modelling of microwave systems, object oriented programming and related topics.